Neoproterozoic Re-Os systematics of organic-rich rocks in the São Francisco Basin, Brazil and implications for hydrocarbon exploration

Maria E. Bertoni[a*], Alan D. Rooney[b,c], David Selby[b], Fernando F. Alkmim[d], Daniel P. Le Heron[a]

[a]Department of Earth Sciences, Queen's Building, Royal Holloway University of London, Egham, Surrey, TW20 0BY, UK

[b]Department of Earth Sciences, Durham University, Durham, DH1 3LE, UK.

[c]Department of Earth and Planetary Sciences, Harvard University, Cambridge, MA, 02138, USA

[d]Departamento de Geologia, Escola de Minas, Universidade Federal de Ouro Preto, Morro do Cruzeiro, 35.400.000 Ouro Preto, MG, Brazil

Abstract

The São Francisco Basin contains a remarkable archive of Neoproterozoic strata and its hydrocarbon-bearing strata are receiving increasing attention as global oil and gas exploration targets progressively deeper and older rocks. New Re–Os geochronology for the Paracatu Slate Formation of the Canastra Group, Brazil yields a depositional age of 1002 ± 45 Ma. This age represents the first successful application of the Re–Os system to rocks of this group and indicates excellent agreement with a previously published U–Pb detrital zircon age (Rodrigues et al., 2010). Together with TOC values of ca. 2 wt.% (despite greenschist metamorphism), it might be argued that the São Francisco Basin has had the potential for hydrocarbon generation since the Tonian (1000 – 850 Ma). In addition, we also report an imprecise Re–Os age (1304 ± 210 Ma) for the Serra do Garrote Formation, a further potential source rock of the Vazante Group. We suggest, based on petrological evidence, that the Re–Os systematics were disturbed by post-depositional fluid flow that was most likely associated with Vazante ore deposit mineralization. An attempt to determine a Re-Os date for the Sete Lagoas Formation, a putative post-Sturtian cap carbonate, is precluded owing to low Re abundances (≤100 ppt). Major environmental changes in the aftermath of the Jequitaí glaciation, particularly the development of palaeotopography such as subglacial tunnel valleys, may account for the apparent random distribution of TOC enrichment in these Cryogenian/Ediacaran post-glacial deposits. This scenario might thus have major implications for the hydrocarbon prospectivity of this post-glacial succession.

Keywords: Re–Os, Neoproterozoic, Canastra, Vazante, Bambuí, source rock

[*]Corresponding author. Tel: +44 (0) 1784 443 581. Postal address: Department of Earth Sciences, Royal Holloway University of London, Egham Hill, Egham, Surrey, TW20 0EX, UK. E-mail addresses: maria.bertoni.2009@live.rhul.ac.uk, bertonime@gmail.com. (M. E. Bertoni)

1. Introduction

The São Francisco Basin and its surrounding belts contain an extensive stratigraphic archive of Proterozoic time, extending at least from the Statherian (1750 Ma) to Late Ediacaran (560 Ma) (Alkmim and Martins-Neto, 2012; Paula-Santos, 2013; Warren et al., 2014). Over a wide area, diamictites and associated cap carbonates have been correlated and linked to major Earth events, as the Sturtian (Babinski and Kaufman, 2003; Azmy et al., 2006; Babinski et al., 2007; Vieira et al., 2007) and Marinoan (Caxito et al., 2012) glacial epochs. In addition, the São Francisco Basin has multiple hydrocarbon gas shows, which are probably sourced from Meso-Neoproterozoic organic-rich rocks (Craig et al., 2013 and references therein). However, the lack of accurate geochronological data throughout the stratigraphy hinders attempts to develop a chronological framework for the São Francisco Basin and its surrounding belts. An understanding of the hydrocarbon potential of these rocks and the relationship of organic-rich horizons to global geological events requires a precise geochronological framework. The absence of volcanic ash layers for U-Pb and Ar-Ar geochronology has hindered attempts to gain absolute geochronological age data (Misi et al., 2011). In addition, age control in these strata is further hampered by the general lack of biostratigraphic constraints, intense deformation and metamorphism. Placing accurate geochronological constraints on organic-rich horizons is integral to understanding of the nature of the depositional environment and fossil hydrocarbon system in this vast basin.

The rhenium–osmium (Re–Os) geochronometer is an increasingly recognized tool for determining depositional ages of organic-rich rocks (Ravizza and Turekian, 1989; Cohen et al., 1999; Selby and Creaser, 2005a; Georgiev et al., 2011; van Acken et al., 2013) and hydrocarbon deposits (Selby et al., 2005; Selby and Creaser, 2005b). The method has yielded absolute dates for Neoproterozoic strata with precision approaching 0.5 % uncertainty (2σ) in units up to greenschist facies (Kendall et al., 2004; Rooney et al., 2014). In the São Francisco Basin of Brazil (**Fig. 1A**) the Re-Os radioisotope system has been previously utilized with limited success to provide depositional ages for the Vazante Group (Geboy, 2006; Azmy et al., 2008; Geboy et al., 2013). Here we evaluate and discuss Re-Os geochronology of the Canastra, Vazante and Bambuí groups with the aim of constraining the depositional age of the organic-rich strata of the Paracatu, Serra do Garrote and Sete Lagoas formations. More widely, this study contributes to the radiometric calibration of the Proterozoic rock record in Brazil, and hence to a better understanding of the geological evolution of the Brasília Belt and São Francisco Basin.

2. Geological setting and existing chronostratigraphy

The São Francisco Craton (**Fig. 1A**) is one of the oldest portions of the Precambrian nucleus of South America (Almeida et al., 2000). Together with the other cratons of South America, it represents the internal portions of plates involved in the assembly of West Gondwana toward the end of the Proterozoic Era (Alkmim and Martins-Neto, 2012). The Brasiliano/Pan-African Orogenic Belts, meanwhile, fringe those ancient plates and also include marginal metasediments accreted during collision (Almeida et al., 2000; Alkmim et al., 2001; Alkmim and Martins-Neto, 2012). The Brasilia Belt, which flanks the São Francisco Basin to the west, exhibits a fundamentally complex tectonic character and variable metamorphic grade. Therefore, it is essential to briefly outline the structural character, the stratigraphy, and present geochronology of both the Brasília Belt and the São Francisco Basin.

"Insert Figure 1 here"

2.1 The Brasilia Belt and São Francisco Basin

The Brasilia Belt, located on the western margin of the São Francisco Craton (**Fig. 1B**), is the product of a collision between the Amazon, São Francisco-Congo and Paranapanema paleocontinents (ca. 850-550 Ma; Pimentel et al., 1999) during the amalgamation of Gondwana (Li et al., 2008; Pimentel et al., 2011; Rodrigues et al., 2012). This belt is composed of thrust sheets verging eastward towards the São Francisco platform (**Fig. 1B**). Metamorphic grade increases progressively westward, reaching granulite facies conditions in the central part of the belt (Dardenne, 2000).

The southern Brasília Belt involves sedimentary rocks grouped into several lithostratigraphic units (**Fig. 1B**): the Araxá, Paranoá, Canastra, and Ibiá groups (Pimentel et al., 2011). Intense deformation, the lack of intercalated volcanic horizons, and the absence of biostratigraphic controls results in multiple possible interpretations for this supracrustal succession (Dardenne, 2000; Valeriano et al., 2008; and references therein). Provenance studies suggest that the Paranoá and Canastra groups are passive margin deposits of the São Francisco paleocontinent, while the Araxá, and Ibiá groups are synorogenic (fore- or back-arc) basin fill (Pimentel et al., 2001; Rodrigues et al., 2010; Pimentel et al., 2011).

The São Francisco Basin occupies the ca. 800 km-long NS-trending lobe of the São Francisco Craton (**Fig. 1A**). Bounded to the west and to the east by emergent thrusts of the adjacent Brasília and Araçuaí Orogenic Belts respectively, the basin is filled by Palaeo-Mesoproterozoic units (Espinhaço Supergroup and Paranoá Group), and Meso-Neoproterozoic strata of the Vazante Group, Jequitaí Formation, and Bambuí Group (Alkmim and Martins-Neto, 2012).

2.2 Canastra Group

The Canastra Group subdivides into three formations (Serra do Landim, Paracatu and Serra dos Pilões). These rocks, which are mainly present in the southern portion of the eastern Brasilia Orogen (**Fig. 1B**), comprise phyllite and quartzite with common carbonate beds (Pereira et al., 1994; Dias, 2011). These have experienced lower greenschist (2-3 kbar and 350-380 °C) facies metamorphism (Freitas-Silva, 1996; Dardenne, 2000). Thrust contacts characterize the boundaries between the Canastra and lower grade metamorphic strata of the Vazante, Paranoá and Bambuí groups (Pereira et al., 1994). It has been suggested that the Canastra Group is a lateral equivalent of the Paranoá Group (Dardenne, 2000; Pimentel et al., 2011).

The lithostratigraphy of the Canastra Group is difficult to unravel owing to numerous thrust faults (Rodrigues et al., 2010) (**Fig. 2**), especially for the basal Serra do Landim Formation (chlorite-rich calc-phyllite and calcschist) and the upper units (Paracatu and the Chapada dos Pilões formations). The Paracatu Formation, which can reach up to ca. 2500 m in thickness (Dias, 2011) comprises slope turbidites and basinal, carbonaceous phyllites rich in diagenetic pyrite, whereas the Chapada dos Pilões Formation consists of shallow marine wave and storm-influenced clastics (Pereira et al., 1994). The coarsening upward succession in the upper Canastra Group thus records a regressive continental platform megasequence (Pereira et al., 1994).

For the Canastra Group, detrital zircon ages reveal Paleoproterozoic (ca. 1.8 and 2.1 Ga) and Mesoproterozoic (1.1-1.2 Ga) peaks, particularly for the Paracatu Formation (Rodrigues et al., 2010). The absence of Neoproterozoic zircon grains related to the active margin of the Brasília Belt, in addition to homogeneous Paleoproterozoic Sm–Nd model ages (ca. 2.2 Ga) (Pimentel et al., 2001) suggests the São Francisco-Congo Craton as the main source region. This led to the interpretation of the Canastra Group as a passive margin succession (Pimentel et al., 2001, 2011). The youngest detrital zircons in the Paracatu Formation are ca. 1040 Ma (Valeriano et al., 2004; Rodrigues et al., 2010; Dias, 2011) (**Fig. 2**); the origin of the Mesoproterozoic (ca. 1.2 Ga) population remains uncertain.

The diagenetic age of the ore-hosting carbonaceous phyllites of the Morro do Ouro Member of the Paracatu Formation has been estimated at 1000-1300 Ma based on Rb-Sr and K-Ar chlorite, and Pb-Pb galena ages (Freitas-Silva, 1996). Metamorphism and gold enrichment of this unit is related to the Brasiliano Event at ca. 680 Ma (Freitas-Silva, 1996).

"Insert Figure 2 here"

2.3 Vazante Group

The Vazante Group positioned in the western margin of the São Francisco Basin (**Fig. 1B**), comprises thick (ca. 5000 m) siliciclastic-dolomite (**Fig. 3**) of marine origin (Azmy et al., 2008; Misi et al., 2011). The Vazante Group is divided into seven formations (Santo Antonio do Bonito, Rocinha, Lagamar, Serra do Garrote, Serra do Poço Verde, Morro do Calcário and Lapa; Dardenne, 2000), which experienced greenschist facies metamorphism. Neoproterozoic Brasiliano thrusts and nappes obscure many sedimentary contacts (Dardenne, 2000), particularly with the Canastra Group to the west and the Bambuí Group to the east (Rodrigues et al., 2012). Intense deformation in the outcrop area raises major uncertainties about the internal stratigraphy and lateral correlation of the units.

In this paper, we analyzed the Serra do Garrote Formation (**Fig. 3**). This formation, which can reach up to 1000 m in thickness (Misi et al., 2011), is dominantly carbonaceous and pyrite-bearing slate, intercalated with fine quartzite beds, representing an open marine succession deposited below storm wave base (Madalosso, 1980). The Serra do Poço Verde Formation lies conformably over the Serra do Garrote Formation and is dominantly dolomitic. The presence of glendonite pseudomorphs after ikaite and dropstones in slates was interpreted as suggestive of paraglacial depositional conditions (Olcott et al., 2005). The Morro do Calcário Formation, a carbonate-stromatolitic succession, often diamictitic (Dardenne, 2000), conformably overlies the former unit. The Morro do Calcário Formation is truncated by an unconformity at the base of the overlying Lapa Formation (Misi et al., 2005), which contains diamictites, organic-rich shale, and cap carbonates with a characteristic negative $\delta^{13}C_{carbonate}$ excursion (ca. -8 to 0 ‰) interpreted to record the resumption of primary productivity in the aftermath of glaciation (Azmy et al., 2006; 2008). A reassessment of the core used by Azmy et al. (2006, 2008) concluded that the unit is part of the Morro do Calcário Formation rather than the Lapa Formation as previously thought (Geboy et al., 2013).

Based on C and Sr isotope profiles, the Morro do Calcário Formation is correlated with the Sturtian glacial epoch (Azmy et al., 2006; ca. 717 Ma; Macdonald et al., 2010). Globally, the chronometry of the Sturtian glaciation is considered to encompass a ca. 60 Myr window, based on U-Pb zircon and Re-Os geochronology of syn- and post-glacial deposits associated with the Rapitan glacial succession in NW Canada (Macdonald et al., 2010; Rooney et al., 2014). However, Re-Os analyses yield Mesoproterozoic depositional ages for organic-rich shales of the Serra do Garrote

(1353 ± 69 Ma) and Serra do Poço Verde (1126 ± 47 Ma) formations, respectively (**Fig. 3**). The same technique together with U-Pb measurements on detrital zircons of the Morro do Calcário Formation, suggest deposition at ca. 1000–1100 Ma (Azmy et al., 2008; **Fig. 3**). As a result, the Vazante Group is considered late Mesoproterozoic, rather than Sturtian (Azmy et al., 2008). Additional, SHRIMP U–Pb detrital zircon analyses (Rodrigues et al., 2012) of five formations of the Vazante Group has identified the youngest population ages (ca. 930 Ma) at the base of the group, and older populations (ranging ca. 1200-1000 Ma) toward the top (**Fig. 3**). A reverse fault identified between the Rocinha and Lagamar formations solve the paradoxical stratigraphic age inversion (Geboy et al., 2013). The same authors also present Re-Os ages for the Serra do Garrote and Morro do Calcário formations of 1354 ± 88 Ma and 1112 ± 50 Ma, respectively (**Fig. 3**).

Despite the complex history of the Vazante Group, the detrital zircon age pattern of the Serra do Garrote Formation (ca. 1.29 Ga, Rodrigues et al., 2012) is coherent with Re-Os isochron ages obtained for the same formation (ca. 1.35 Ga, Geboy, 2006; Geboy et al., 2013). However, high Mean Square of Weighted Deviates (MSWD) values of 26 and 49 is associated with these Re-Os isochrons rendering them imprecise and less than conclusive with regards to the true age of the Vazante Group (Geboy, 2006; Geboy et al., 2013). Therefore, further provision of radiometric ages is clearly necessary, and motivates our attempts to date the Serra do Garrote Formation.

"Insert Figure 3 here"

2.4 Neoproterozoic glacials and the Jequitaí Formation

Evidence for glaciation in the Jequitaí Formation in the São Francisco Basin and its correlatives, the Bebedouro Formation (northern São Francisco Craton) and Macaúbas Group (Araçuaí Belt), is compelling (e.g. Cukrov et al., 2005; Uhlein et al., 2007; Chaves et al., 2010). The preceding authors reported a striated pavement cut into the Espinhaço Supergroup in the northeastern portion of the São Francisco Basin, together with abundant diamictites with exotic lonestones, some of which are well stratified and exhibit unequivocal impact structures implying ice-rafted debris. Furthermore, on the western margin of the São Francisco Basin, Martins-Ferreira et al. (2013; **Fig. 1**) describe a ca. 4 km-wide valley carved in sandstone of the Paranoá Group and filled by a ca. 40 m package of sandstone, diamictite and tillite of the Jequitaí Formation. These glaciogenic rocks are, in turn, covered by a cap carbonate that marks the base of the Bambuí Group in the São Francisco Basin (**Fig. 4**). With the exception of the striated pavement, each of these facies are recognised in proprietary cores across the subsurface of the basin. Zircons U-Pb systematics extracted from the Jequitaí Formation and the correlative Macaúbas Group yield maximum deposition ages of 880 Ma and 864 Ma, respectively (Pedrosa-Soares et al., 2000; Rodrigues et al., 2008).

2.5 Bambuí Group

These epicontinental deposits, of alternating siliciclastics and carbonates are the most widely distributed unit in the São Francisco Basin (**Fig. 1**), draping the Jequitaí diamictites and sandstones. They form a shallowing upwards sequence (Dardenne, 2000; Santos et al., 2000), divisible into three coarsening upward megacycles (Dardenne, 2000; Martins-Neto, 2009). The first megacycle is represented by the Sete Lagoas Formation, the second includes the Serra de Santa Helena and Lagoa do

Jacaré formations and the last cycle comprises the Serra da Saudade and Três Marias formations (Martins and Lemos, 2007) (**Fig. 4**). The absence of volcanic ash horizons throughout the Bambuí Group, in addition to hampering geochronology, has promoted debate regarding the tectonic setting for this group (e.g. Alkmim and Martins-Neto, 2001; Zalán and Silva, 2007) and its relationship with the Jequitaí diamictites (Babinski et al., 2007, 2012; Misi et al., 2011; Caxito et al., 2012).

The Sete Lagoas Formation, for which we present data in this paper, comprises a ca. 200 m succession (Vieira et al., 2007) of siliciclastic-calcareous sediments, grading upwards into microcrystalline limestones and dolostones. Its upper section contains the most extensive shallow water carbonates of the basin with laminated and columnar *Gymnosolenide* stromatolites (Dardenne, 1978) and evidence for subaerial exposure (Martins and Lemos 2007). Its basal contact is characterized by an unconformity: the formation rests on granite-gneiss basement, on the glaciogenic Jequitaí Formation, or on conglomerates of the Carrancas Formation, exposed along the southern border of the basin (Dardenne, 2000, Alkmin and Martins-Neto, 2001, Vieira et al., 2007).

Several isotopic studies have demonstrated a negative excursion of $\delta^{13}C_{carbonate}$ (ca. -4 to 0 ‰) for the base of the Sete Lagoas Formation (e.g. Alvarenga et al., 2007; Kuchenbecker, 2011). The $\delta^{13}C$ signature, together with its stratigraphic position, sitting on top of the Jequitaí diamictite deposits, has led to interpretations of a typical postglacial cap carbonate sequence related either to Sturtian (Babinski and Kaufman, 2003; Babinski et al., 2007; Vieira et al., 2007) or Marinoan (Caxito et al., 2012) deglaciation. Despite a large suite of isotopic and chemostratigraphic data available the depositional age has been unknown until recently. A Pb-Pb age of 740 ± 22 Ma (**Fig. 4**) from basal carbonates of the Sete Lagoas Formation (Babinski et al., 2007) was the first estimate for its depositional age. Subsequently, U-Pb detrital zircons in siliciclastics intervals provided maximum depositional ages of 610 Ma (Rodrigues, 2008) and 557 Ma (Paula-Santos, 2013) (**Fig. 4**). An Ediacaran fossil assemblage containing *Cloudina sp*. has recently been discovered in the central-eastern part of the basin (from the middle part of the Sete Lagoas Formation) (**Fig. 4**): this suggests a narrow time window (ca. 550-542 Ma) on account of the known global biozone that this assemblage represents (Warren et al., 2014 and references therein).

"Insert Figure 4 here"

From the above, it is clear that the depositional age of the Sete Lagoas Formation spans ca. 200 Myr. Thus, the different ages may imply that this formation contains a substantial hiatus within it. On the other hand, identical $^{87}Sr/^{86}Sr$ values (0.7074-0.7076) obtained both below and above the supposed unconformity separating the Cryogenian from the Ediacaran carbonates, argue against this hypothesis (Caxito et al., 2012).

In view of the uncertainties described earlier, and the necessity of understanding the context of deposition of the Bambuí Group, further provision of radiometric ages are required. In addition, most of the geochronological determinations derive from outcrops along the eastern margin of the basin (Babinski et al., 2007; Rodrigues, 2008; Paula-Santos, 2013). Thus, access to core material from the southwestern margin in the present study will extend knowledge to other parts of the carbonate platform.

3. Methods

3.1 Sampling

Samples of the 3 formations in this study were collected from proprietary drill cores (**Fig. 1**). Drill cores intersecting the Paracatu and Serra do Garrote formations were provided by Votorantim Mine and a mining company from the Arcos region supplied the Sete Lagoas Formation samples. In the MASW03 (Paracatu Formation) core (**Fig. 5A**) the sampled interval spans 47.10 to 55.70 m (MD) and include dark grey to black slates, with sporadic quartz as thin veins together with pyrite. VZCF001 (Serra do Garrote Formation) core samples (**Fig. 5B**) extend from 280.10 to 292.65 m and include black slates, with considerable carbonaceous material (staining). Pyrite is present, both as lamina-parallel mineralization, and as crosscutting veins and framboid nodules. Finally, LMR1009 (Sete Lagoas Formation) core samples (**Fig. 5C**) were obtained from four intervals; 1, from 36-47 m (microbial dolomite and mudstones); 2, from 111-118 m (laminated limestones with carbonaceous seams); 3, from 144-157 m (clay-rich limestones); 4, from 158-165 m (argillites). Following Kendall et al. (2009a), ca. 100g samples were collected at 1 m intervals in each core. Sub-sampling at further 0.4 m intervals was undertaken to detect further changes in Re and Os abundance and isotope composition.

We note that petrographic inspection of the Serra do Garrote Formation in core VZCF001 revealed faulting, brecciation of the host rock and pervasive quartz veining. Care was taken to avoid these zones of hydrothermal alteration and mineralization.

3.2 Total organic carbon (TOC)

TOC values for the all samples were determined at the School of Civil Engineering and Geoscience of Newcastle University, UK. An accurately weighed 0.1 g of powdered rock was digested in hot (60-70 °C) hydrochloric acid (4 mol/L) to remove the inorganic (carbonate) carbon. The decarbonated and washed samples (in deionised water) were then dried overnight in an oven at 65 °C. The organic carbon in the decarbonated samples was determined using a Leco CS230 Carbon-Sulphur analyser (previously calibrated on standard samples; standard deviation 3 %).

3.3 Re-Os geochronology

For Re-Os analysis, the core samples were polished using a diamond coated polishing pad to eliminate any metal contamination (e.g. cutting and drilling marks). Each sample was dried at 60 °C for 24 h and then crushed to a powder (c. 30 µm) in a zirconium dish using an automated shatterbox. Re and Os isotope analyses were carried out at Durham University's TOTAL laboratory for source rock geochronology and geochemistry at the Northern Centre for Isotopic and Elemental Tracing (NCIET) using methods outlined in Selby and Creaser (2003) and Selby (2007). Between 0.2 and 0.4 g of each sample was digested and equilibrated in a borosilicate carius tube in 8 ml of Cr^{VI}–H_2SO_4 together with a mixed tracer (spike) solution of ^{190}Os and ^{185}Re at 220 °C for 48 h. The Cr^{VI}–H_2SO_4 solution was used to liberate hydrogenous Re and Os, restricting the incorporation of non-hydrogenous Re and Os (Kendall et al., 2004). Solvent extraction ($CHCl_3$) for Re and Os purification, micro-distillation and anion chromatography methods were employed as outlined by Cumming et al. (2013). The purified Re and Os fractions were loaded onto Ni and Pt filaments, respectively (Selby, 2007), with the isotopic measurements determined by Negative Thermal Ionization Mass Spectrometry using a ThermoScientific mass spectrometer via static Faraday collection for Re and ion-counting using a secondary electron multiplier in peak-hopping mode for Os. Total procedural blanks during this study were 14.6 ±

0.16 pg and 0.05 ± 0.01 pg (1σ S.D., *n* = 3) for Re and Os, respectively, with an average ^{187}Os/^{188}Os value of 0.61 ± 0.03 (*n* = 3). Uncertainties for ^{187}Re/^{188}Os and ^{187}Os/^{188}Os were determined by error propagation of uncertainties in Re and Os mass spectrometer measurements, blank abundances and isotopic compositions, spike calibrations and reproducibility of standard Re and Os isotopic values. The Re–Os isotopic data including the 2σ calculated uncertainties for ^{187}Re/^{188}Os and ^{187}Os/^{188}Os and the associated error correlation function (rho) were regressed to yield a Re–Os date using Isoplot V. 4.0 and the λ ^{187}Re constant of 1.666×10^{-11} a^{-1} (Smoliar et al., 1996; Ludwig, 2003). The age uncertainty including the uncertainty of 0.35 % in the ^{187}Re decay constant only affects the third decimal place (Smoliar et al., 1996; Selby, 2007).

To evaluate mass spectrometry reproducibility, two in-house Re and Os (Durham Romil Osmium Standard=DROsS) solution standards were analyzed. The Re solution standard yields an average ^{185}Re/^{187}Re ratio of 0.598071 ± 0.001510 (1 S.D., *n* = 67), which is in agreement with the value reported for the AB-1 standard (Rooney et al., 2010). The measured difference in ^{185}Re/^{187}Re values for the Re standard solution and the accepted ^{185}Re/^{187}Re value (0.5974; Gramlich et al., 1973) is used to correct the measured sample Re isotope composition. The Os isotope reference solution (DROsS) gave an ^{187}Os/^{188}Os ratio of 0.160892 ± 0.000559 (1 S.D., *n* = 67), which is in agreement with previous studies (Rooney et al., 2010).

4. Results

4.1 TOC

The TOC results for all samples are presented in **Table 1** and **Fig. 5A, B and C**. The Sete Lagoas Formation has the lowest TOC of the 3 analyzed cores (<0.01 to 0.49

wt%), while the Serra do Garrote and Paracatu formations possess the highest TOC values (0.75 to 2.12 wt % and 0.07 to 2.15 wt %, respectively). According to these samples, the basin possesses fair quality as a potential hydrocarbon source rock, both in carbonates and shales (c.f. Craig et al., 2013). Re-Os geochronology has been applied successfully to rocks with < 0.5 % TOC (Kendall et al., 2004), thus this cut off value was used to select the samples for Re-Os analysis. Only the samples from the Paracatu and Serra do Garrote formations provided ≥1 wt% TOC (**Fig. 5A** and **B**), in low-grade metamorphic rocks. Therefore, maturation analyses (Rock Eval) were not performed.

"Insert Table 1 here"

"Insert Figure 5 here"

4.2 Paracatu Slate Formation: Re-Os data

The Paracatu Slate Formation samples have Re (0.3 – 4.1 ppb) and Os (53 – 297 ppt) abundances (**Table 2**) that are close to or less than that of average continental crustal values of 1 ppb and 50 ppt, respectively (Esser and Turekian, 1993; Peucker-Ehrenbrink and Jahn, 2001; Hattori et al., 2003). The $^{187}Re/^{188}Os$ ratios display a limited range from 24.2 to 79.6 and present-day $^{187}Os/^{188}Os$ ratios range from 0.667 to 1.593 (**Table 2**). Regression of the Re–Os isotope data yield a Re–Os age of 1002 ± 45 Ma (2σ, n = 4, Model 1, MSWD = 1.2, initial $^{187}Os/^{188}Os$ = 0.25 ± 0.04; **Fig. 6A**). This initial $^{187}Os/^{188}Os$ (hereafter Os_i) value is remarkably unradiogenic and will be discussed further in the following section.

"Insert Table 2 here"

"Insert Figure 6 here"

4.3 Serra do Garrote Formation: Re-Os data

The Serra do Garrote slates are enriched in Re (4 - 28 ppb) and Os (137 - 585 ppt; **Table 2**) and present a large spread in $^{187}Re/^{188}Os$ ratios (205.1 - 601.2) and $^{187}Os/^{188}Os$ ratios (3.628 - 12.207) (**Fig. 6B**). Replicate analysis of one Serra do Garrote sample (VZCF-6r) show good reproducibility in Re and Os abundances and $^{187}Re/^{188}Os$ and $^{187}Os/^{188}Os$ ratios. Contrary to the Paracatu Slate Formation, regression of the isotopic composition data for the Serra do Garrote Formation yield an imprecise, Model 3 age of 1304 ± 210 Ma (MSWD = 96), with a negative initial Os isotope value of -1.0 ± 1.4.

4.4 Sete Lagoas Formation: Re-Os data

The samples of the Sete Lagoas Formation have very low Re abundances <100 ppt, which are lower than estimated average (present-day) upper continental crust. These samples are not amenable to Re-Os geochronology as the low Re abundances would result in very large (>100 %) uncertainties in isotopic measurements using current analytical techniques.

5. Discussion

5.1 Paracatu Slate Formation

New Re–Os geochronology for the Paracatu Slate Formation yields a depositional age of 1002 ± 45 Ma, which agrees, within uncertainty, with U–Pb geochronology data (detrital zircons ca. 1040 Ma; Valeriano et al., 2004; Rodrigues et al., 2010; Dias, 2011). This relatively precise age represents the first successful application of the Re–

Os geochronometer in samples of the Canastra Group. The new Re–Os geochronology data adds credence to previous studies that suggest that there is no significant disturbance in the Re-Os systematics of carbonaceous organic-rich rocks that have experienced anhydrous greenschist facies metamorphism (Kendall et al., 2004; Rooney et al., 2011).

The Os_i value for seawater at the time of deposition of the Paracatu Formation (0.25 ± 0.04) is much less radiogenic than that of modern-day seawater (ca. 1.06; Levasseur et al., 1998) indicating that the dominant input of Os to seawater was non-radiogenic. This Os_i value is consistent with a marine Os budget dominated by extraterrestrial and ultramafic-mafic magmatic/hydrothermal inputs with minor contribution of radiogenic Os from continental weathering sources. The calculated Os isotope composition of continental crust at 1 Ga ranges from 0.5-1.0 thus indicating that this source played a minor role in the oceanic budget during this time as has been previously postulated (Kendall et al., 2009a; Rooney et al., 2010; van Acken et al., 2013). The Paracatu Slate Formation Os_i value provides an additional data point to the record for Precambrian seawater, evidencing that the change in global patterns of oxidative weathering and Os influx was of little importance, at least until the earliest Tonian (van Acken et al., 2013) although this remains contentious (Sperling et al., 2014).

Based on our Re-Os data, the Canastra Group was deposited at or around the Meso-Neoproterozoic boundary. This places the Canastra Group as a possible correlative of the Paranoá Group, considering the diagenetic xenotime U-Pb age of 1042 ± 22 Ma of the latter (Matteini et al., 2012). Moreover, the Re-Os age endorses tectonostratigraphic models of a passive margin sequence, deposited along the SW margin of the São Francisco-Congo paleocontinent (Pimentel et al., 2001, 2011;

Rodrigues et al., 2010). As the detrital zircons and depositional Re-Os isochron of the Canastra Group are similar, this requires the rapid exhumation of the Mesoproterozoic source region (main peak at ca. 1.2 Ga (Stenian); Rodrigues et al., 2010). On the other hand, the youngest zircon population of the Paranoá Group interpreted as a maximum depositional age (1540 Ma (Calymmian); Matteini et al., 2012) necessarily imposes source isolation later in the evolution of the passive margin, if both units are indeed chrono-correlatives.

Considering the amount of organic matter preserved even after maturation (ca. 2 wt %,), it is likely that the Paracatu Slate Formation of the Canastra Group constituted an extensive hydrocarbon source rock. Despite no remaining potential for further hydrocarbon generation, it is not implausible that between deposition (ca. 1000 Ma) and prior to the last tectono-metamorphic event recognised in the Brasília Belt (ca. 600 Ma; Pimentel et al., 1999), the rock expelled hydrocarbons. However, the presently available data is insufficient to determine the precise timing of hydrocarbon generation/migration, as the intense deformation during the Neoproterozoic Brasiliano Event and the posthumous erosion has obliterated true stratigraphic thicknesses.

5.2 Serra do Garrote Formation

The Serra do Garrote Formation, which similarly to the Paracatu Formation has experienced regional Brasiliano metamorphism (Dardenne, 2000), shows a large scatter about the Re–Os regression line (Model 3, 1304 ± 210, MSWD = 96) together with a negative initial Os isotope composition (-1.0 ± 1.4) suggestive of disturbances to the Re–Os systematics. This imprecise age may result from either depositional and/or post-depositional processes. The presence of detrital Os with variable

$^{187}Os/^{188}Os$ values, may result in imprecise and geologically meaningless ages (Kendall et al., 2004, 2009a), but is considered an unlikely cause because the Cr^{VI}-H_2SO_4 digestion technique preferentially liberates hydrogenous Os. Another feasible cause of geological uncertainty for the Re-Os systematics may be variations in initial Os isotope compositions during deposition (Selby and Creaser, 2003). In order to avoid these heterogeneities, short stratigraphic sampling intervals (ca. 0.6 m) were employed. The Os isotope composition of the Serra do Garrote Formation, however, show variations that exceed those expected from temporal evolution in seawater (unless sedimentation rates were anomalously low). Thus, these variations do not fully account for the complex Re–Os systematics in the Serra do Garrote Formation.

Weathering and metamorphism are unlikely explanations for the scattered Re-Os isotope systematics because drill core provided access to material showing no apparent evidence of surficial alteration. Additionally, metamorphic conditions of the Serra do Garrote Formation related to the Brasiliano Orogeny did not exceed greenschist facies (Dardenne, 2000; Misi et al., 2005, 2007). Petrological evidence (coarse pyrite aggregates, quartz veinlets and pervasive faulting and fracturing) suggests the Serra do Garrote Formation has been affected by hydrothermal fluid flow. Although we avoided sampling material with abundant quartz veins, the scatter in the Re–Os regressions for the Serra do Garrote Formation and the Os_i signature of the samples is indicative of a hydrothermal alteration origin, implying that there might have been some mobilization of Re and Os by fluid flow. Similar Re-Os behaviour has been observed by Rooney et al. (2011) for the Leny Limestone and by Kendall et al. (2009b) for the Wollogorang Formation. Although the Vazante Ore hypogene deposit is located in the overlying Serra do Poço Verde Formation (Monteiro et al., 2006), we do not discount the possibility that the same mineralizing and oxidizing fluids may have affected the Serra do Garrote Formation due to the proximity of well VZCF001 to brecciated metadolomites and epigenetic willemitic ore bodies along the Vazante Shear Zone (**Fig. 1B**). Therefore, it is possible that the high-temperature (> 250 °C), oxidizing and moderate saline (ca. 15 wt. % NaCl equiv.) brines that leached base metals from the basement and ascended to finally interact with the host dolostones of the Serra do Poço Verde (Monteiro et al., 2003; Misi et al., 2005) have hydrated the Serra do Garrote slates, resulting in disturbance of the Re–Os geochronometer. Similar alteration of Re-Os systematics by mineralizing fluid circulation might also explain why previous attempts to date the Serra do Garrote and Morro do Calcario formations with the Re-Os geochronometer (Geboy, 2006; Azmy 2008; Geboy et al., 2013) were unsuccessful.

It is likely that the extensive hydrothermal activity recorded in the Vazante Group, and associated with the abundant Zn deposits (Monteiro et al., 2006) had intrinsic relation with hydrocarbon generation, possibly sourced by the Serra do Garrote Formation. Pyrobitumen has been observed within hydrothermal veins in the carbonates of the overlying Morro do Calcário Formation (Rubo and Monteiro, 2010; Tonietto, 2011) and hydrocarbon inclusions were described in sulfides of the Vazante ore deposit (L. Monteiro *pers. comm.*). Future dating of these hydrocarbon products with the ^{187}Re-^{187}Os radioisotope system (e.g., Selby and Creaser, 2005b) could help constraining the timing of emplacement, the source of migrated hydrocarbons and the temporal relation of the mineralization and hydrocarbon accumulation.

5.3 Sete Lagoas Formation

The low Re and Os abundance in the carbonate of the Sete Lagoas could be intrinsically associated with the low TOC observed for the unit, and/or be directly related to the depositional environment and the organic matter type (Colodner et al., 1993; Crusius and Thomson, 2000; Selby and Creaser, 2003; Cumming et al., 2012; Harris et al., 2013). Further, the observed low organic content can also be related to thermal maturation (Peters and Cassa, 1994) which may cause a loss of 30-50 % of the assumed original amount of TOC (Buchardt et al., 1986). Despite the intention of accounting for the effects of maturation using biomarker studies, the results proved inconclusive likely due to low volumes of organic matter analysed.

The recognition of palaeovalleys in outcrop (Martins-Ferreira et al., 2013), and information of their infill with the Jequitaí Diamictites and post-glacial cap Bambuí carbonate may have important implications for the distribution of organic-rich facies. If indeed the Jequitaí glaciation left a sculpted palaeotopography, then factors linked to restricted/open circulation within/out palaeovalleys may explain oxic versus anoxic conditions for organic preservation and associated Re and Os complexation. The lack of diamictites underlying carbonates of the Sete Lagoas Formation in well LMR1009 (opposed to other cores of the region; F. Pimenta *pers. comm.*; Kuchenbecker 2011; Kuchenbecker et al., 2011, 2013) could indicate a distal position from paleodepressions, resulting in the low TOC values observed in this particular location. This interpretation can only be tentative, however, because seismic sections are not yet available in this region. Nevertheless, considering that similar distributions are recognised in other Neoproterozoic post-glacial successions (Bechstädt et al., 2009), and that organic-rich post-glacial facies in North Africa have charged more than 50 major oil and gas fields (Lüning et al., 2000), the Sete Lagoas Formation may yet have good source rock potential. Further studies are clearly required to unravel the complex depositional history of this unit.

6. Conclusions

New Re–Os geochronology for the Paracatu Slate Formation yields a depositional age of 1002 ± 45 Ma and is in agreement, within uncertainty, of U–Pb detrital geochronology. This relatively precise age provides a more precise chronostratigraphic framework for understanding the tectonic evolution of the Canastra Group and the onset of sedimentation within the São Francisco Basin.

Disturbance of Re–Os systematics in the Serra do Garrote Formation is evident by an imprecise and inaccurate age along with a negative value for the Os_i value. These factors together with petrological evidence strongly suggest that the Re–Os system was disturbed in response to hydrothermal fluid flow, possibly associated with the Vazante ore deposit mineralization events. The circulation of oxygenated fluids through the Vazante Group is suggested to be the cause for disturbance to the Re-Os geochronometer. Consequently, care is necessary when applying the Re–Os deposition-age geochronometer to sedimentary rocks that have experienced tectonic deformation and hydrothermal fluid flow.

The lack of Re enrichment in the base of the Sete Lagoas Formation could be explained by the distribution of the organically-rich facies which, similarly to the deglacial shales in North Africa (Lüning et al., 2000), was inherited from glacial topography.

Acknowledgements

This research was generously funded by a grant from Sonangol to Daniel P. Le Heron, supporting the doctoral research of the first author and the AAPG Foundation Gordon I. Atwater Grant awarded to MEB. The Brazilian Council for Scientific and

Technological Development- CNPq provided a reaserch grant to F. F. Alkmim (Grant#307531/2009-0). Votorantim mine and a mining company from Arcos region, are thanked for provision of core samples and particular Samuel Boucas do Lago, Gustavo Diniz Oliveira, Felipe Pimenta and Leonardo Lopes-Silva are thanked for their assistance with the sample collection. Comments from two anonymous reviewers greatly improved this paper.

References

Alkmim, F. F., and Martins-Neto, M. A., 2001. A Bacia intracratônica do São Francisco: Arcabouço estrutural e cenários evolutivos. Bacia do São Francisco: geologia e recursos naturais. SBG-MG, Belo Horizonte, 9-30.

Alkmim, F. F., Marshak, S., and Fonseca, M. A., 2001. Assembling West Gondwana in the Neoproterozoic: clues from the São Francisco craton region, Brazil. Geology, 29(4), 319-322.

Alkmim, F. F., and Martins-Neto, M. A., 2012. Proterozoic first-order sedimentary sequences of the São Francisco craton, eastern Brazil. Marine and Petroleum Geology, 33(1), 127-139.

Almeida, F. F. M. D., Brito Neves, B. B. D., and Dal Ré Carneiro, C., 2000. The origin and evolution of the South American Platform. Earth-Science Reviews, 50(1), 77-111.

Alvarenga, C. J. S., Della Giustina, M. E. S., Silva, M. G. C., Santos, R. V., Gioia, S. M. C., Guimarães, E. M., Dardenne, M. A., Sial, A. N., Ferreira, V. P., 2007. Variacões dos isótopos de C e Sr em carbonatos pré e pós-glaciacão Jequitaí (Esturtiano) na região de Bezerra-Formosa, Goiás. Revista Brasileira de Geociências 37, 147-155.

Azmy, K., Kaufman, A. J., Misi, A., and Oliveira, T. F. D., 2006. Isotope stratigraphy of the Lapa formation, São Francisco Basin, Brazil: implications for late Neoproterozoic glacial events in South America. Precambrian Research, 149(3), 231-248.

Azmy, K., Kendall, B., Creaser, R. A., Heaman, L., and de Oliveira, T. F., 2008. Global correlation of the Vazante Group, São Francisco Basin, Brazil: Re–Os and U–Pb radiometric age constraints. Precambrian Research, 164(3), 160-172.

Babinski, M., Kaufman, A. J., and Varni, M., 2003. First direct dating of a Neoproterozoic post-glacial cap carbonate. South American Symposium on Isotope Geology. 4, 321-323.

Babinski, M., Vieira, L. C., and Trindade, R. I., 2007. Direct dating of the Sete Lagoas cap carbonate (Bambuí Group, Brazil) and implications for the Neoproterozoic glacial events. Terra Nova, 19(6), 401-406.

Babinski, M., Pedrosa-Soares, A. C., Trindade, R. I. F., Martins, M., Noce, C. M., and Liu, D., 2012. Neoproterozoic glacial deposits from the Araçuaí orogen, Brazil: Age, provenance and correlations with the São Francisco craton and West Congo Belt. Gondwana Research, 21(2), 451-465.

Bechstädt, T., Jäger, H., Spence, G. and Werner, G., 2009. Late Cryogenian (Neoproterozoic) glacial and post-glacial successions at the southern margin of the Congo Craton, northern Namibia: facies, palaeogeography and hydrocarbon perspective. In: Craig, J., Thurow, J., Thusu, B., Whitham, A. and Abutarruma, Y. (eds) Global Neoproterozoic Petroleum Systems: The Emerging Potential in North Africa. Geological Society, London, Special Publications, 326, 255-287.

Buchardt, B., Clausen, J., and Thomsen, E., 1986. Carbon isotope composition of Lower Palaeozoic kerogen: effects of maturation. Organic geochemistry, 10(1), 127-134.

Caxito, F. D. A., Halverson, G. P., Uhlein, A., Stevenson, R., Gonçalves Dias, T., and Uhlein, G. J., 2012. Marinoan glaciation in east central Brazil. Precambrian Research, 200, 38-58.

Chaves, M. L. D. S. C., Guimarães, J. T., and Andrade, K. W. 2010. Glaciomarine lithofacies in the Jequitaí Formation: possible implications for the redistribution of diamonds to the west of the Espinhaço Range (MG). Revista Brasileira de Geociências, 40(4), 516-526.

Cohen, A. S., Coe, A. L., Bartlett, J. M., and Hawkesworth, C. J. 1999. Precise Re–Os ages of organic-rich mudrocks and the Os isotope composition of Jurassic seawater.

Earth and Planetary Science Letters, 167(3), 159-173.

Colodner, D., Sachs, J., Ravizza, G., Turekian, K., Edmond, J and Boyle, E., 1993. The geochemical cycle of rhenium: a reconnaissance. Earth and Planetary Science Letters, **117,** 205-221.

Craig, J., Biffi, U., Galimberti, R. F., Ghori, K. A. R., Gorter, J. D., Hakhoo, N., Le Heron, D. P., Thurow, J., Vecoli, M., 2013. The palaeobiology and geochemistry of Precambrian hydrocarbon source rocks. Marine and Petroleum Geology, 40, 1-47.

Crusius, J., and Thomson, J., 2000. Comparative behavior of authigenic Re, U, and Mo during reoxidation and subsequent long-term burial in marine sediments. Geochimica et Cosmochimica Acta, **64,** 2233-2242.

Cukrov, N., De Alvarenga, C. J. S. and Uhlein, A., 2005. Litofácies da glaciação Neoproterozóica nas porções sul do cráton do São Francisco: Exemplos de Jequitaí (MG) e Cristalina (Go). Revista Brasileira de Geociências, 35, 69-76.

Cumming, V. M., Selby, D., and Lillis, P. G., 2012. Re–Os geochronology of the lacustrine Green River Formation: Insights into direct depositional dating of lacustrine successions, Re–Os systematics and paleocontinental weathering. Earth and Planetary Science Letters, 359, 194-205.

Cumming, V.M, Poulton, S.W., Rooney, A.D. and Selby, D., 2013. Anoxia in the terrestrial environment during the Late Mesoproterozoic. Geology 41(5), 583-586.

Dardenne, M. A., 1978. Síntese sobre a estratigrafia do Grupo Bambuí no Brasil Central. SBG, Congresso Brassileiro de Geologia, 30, 507-610.

Dardenne, M. A., 2000. The Brasília fold Belt. In: Cordani, U. G., Milani, E. J., Thomaz Filho, A., Campos, D. A. (Eds.), Tectonic Evolution of South America. 31st International Geological Congress, Rio de Janeiro, 231-263.

Dias, P. H. A., 2011. Estratigrafia dos grupos Canastra e Ibiá (Faixa Brasília Meridional) na região de Ibiá, Minas Gerais: caracterização e estudo de proveniência sedimentar com base em estudos isotópicos U-Pb e Sm-Nd. Master Thesis, Federal University of Minas Gerais. Belo Horizonte, 92 p..

Esser, B. K., and Turekian, K. K., 1993. The osmium isotopic composition of the continental crust. Geochimica et Cosmochimica Acta, 57(13), 3093-3104.

Freitas-Silva, F. H., 1996. Metalogênese do depósito do Morro do Ouro, Paracatu, MG. Doctoral Thesis, University of Brasília. Brasília, 339 p..

Geboy, N. J., 2006. Rhenium-Osmium Age Determinations of Glaciogenic Shales from the Mesoproterozoic Vazante Formation, Brazil. Master Thesis, Maryland University. Maryland, 91 p..

Geboy, N. J., Kaufman, A. J., Walker, R. J., Misi, A., de Oliviera, T. F., Miller, K. E., Azmy, K., Kendall, B., and Poulton, S. W., 2013. Re–Os age constraints and new observations of Proterozoic glacial deposits in the Vazante Group, Brazil. Precambrian Research, 238, 199-213.

Georgiev, S., Stein, H. J., Hannah, J. L., Bingen, B., Weiss, H. M., and Piasecki, S., 2011. Hot acidic Late Permian seas stifle life in record time. Earth and Planetary Science Letters, 310(3), 389-400.

Gramlich, J. W., Murphy, T. J., Garner, E. L., Shields, W. R., 1973. Absolute isotopic abundance ratio and atomic weight of a reference sample of rhenium. Journal of Research of the National Bureau of Standards, 77A, 691–698.

Harris, N. B., Mnich, C. A., Selby, D., Korn, D., 2012. Minor and Trace Element and Re-Os Chemistry of the Upper Devonian Woodford Shale, Permian Basin, West Texas: Insights into Metal Abundance and Basin Processes. Chemical Geology, 356, 76-93.

Hattori, Y., Suzuki, K., Honda, M., and Shimizu, H., 2003. Re-Os isotope systematics of the Taklimakan Desert sands, moraines and river sediments around the Taklimakan Desert, and of Tibetan soils. Geochimica et cosmochimica acta, 67(6), 1203-1213.

Kendall B. S., Creaser R. A., Ross G. M. and Selby D., 2004. Constraints on the timing of Marinoan ‘‘Snowball Earth” glaciation by ^{187}Re–^{187}Os dating of a Neoproterozoic, post- glacial black shale in Western Canada. Earth Planetary Science Letters 222, 729–740.

Kendall, B., Creaser, R. A., and Selby, D., 2009a. ^{187}Re-^{187}Os geochronology of Precambrian organic-rich sedimentary rocks. Geological Society, London, Special Publications, 326(1), 85-107.

Kendall, B., Creaser, R. A., Gordon, G. W., and Anbar, A. D. 2009b. Re–Os and Mo isotope systematics of black shales from the Middle Proterozoic Velkerri and Wollogorang formations, McArthur Basin, northern Australia. Geochimica et Cosmochimica Acta, 73(9), 2534-2558.

Kuchenbecker, M., 2011. Quimioestratigrafia e proveniência sedimentar da porc¸ ão basal do Grupo Bambuí em Arcos (MG). Master Thesis, Federal University of Minas Gerais. Belo Horizonte, 91 p..

Kuchenbecker, M., Lopes-Silva, L., Pimenta, F., Pedrosa-Soares, A. C., and Babinski, M., 2011. Estratigrafia da porção basal do grupo Bambuí na região de Arcos (MG): uma contribuição a partir de testemunhos de sondagem. Geologia USP. Série Científica, 11(2), 45-54.

Kuchenbecker, M., Babinski, M., Pedrosa-Soares, A. C., Costa, R. D. D., Lopes-Silva, L., and Pimenta, F., 2013. Proveniência e análise sedimentar da porção basal do Grupo Bambuí em Arcos (MG). Geologia USP. Série Científica, 13(4), 49-61.

Levasseur, S., Birck, J. L. and Allègre, C. J., 1998. Direct measurement of femtomoles of osmium and the ^{187}Os/^{186}Os ratio in seawater. Science, 282(5387), 272-274.

Li, Z. X., Bogdanova, S. V., Collins, A. S., Davidson, A., De Waele, B., Ernst, R. E., Fitzsimons, I. C. W., Fuck R. A., Gladkochub, D. P., Jacobs, J., Karlstrom, K. E., Lu S., Natapov, L. M., Pease, S. A., Pisarevsky, S. A., Thrane, K., and Vernikovsky, V., 2008. Assembly, configuration, and break-up history of Rodinia: a synthesis. Precambrian Research, 160(1), 179-210.

Ludwig, K., 2003. Isoplot/Ex, Version 3: A Geochronological Toolkit for Microsoft

Lüning, S., Craig, J., Loydell, D. K., Storch, P. and Fitches, W., 2000. Lowermost Silurian 'hot shales' in north Africa and Arabia: regional distribution and depositional model. Earth Science Reviews, 49, 121–200.

Macdonald, F. A., Schmitz, M. D., Crowley, J. L., Roots, C. F., Jones, D. S., Maloof, A. C., Strauss, J. V., Cohen, P. A., Johnston, D. T., and Schrag, D. P., 2010. Calibrating the Cryogenian. Science, 327(5970), 1241-1243.

Madalosso, A., 1980. Considerações sobre a paleogeografia do Grupo Bambuí na região de Paracatu – Morro Agudo (MG). In: 31 Congresso Brasileiro de Geologia, Anais, (2), 772-785.

Martins, M., and Lemos, V. B., 2007. Análise estratigráfica das seqüências neoproterozóicas da Bacia do São Francisco. Brazilian Journal of Geology, 37(4), 156-167.

Martins-Ferreira, M. A., Campos, J. E. G. and Alvarenga, C. J. S. 2013. A Formação

Jequitaí na região de Vila Boa, GO: exemplo de sedimentação por geleiras terminais no Neoproterozóico. Brazilian Journal of Geology, 43(2), 373-384.

Martins-Neto, M. A., 2009. Sequence stratigraphic framework of Proterozoic successions in eastern Brazil. Marine and Petroleum Geology, 26(2), 163-176.

Matteini, M., Dantas, E. L., Pimentel, M. M., de Alvarenga, C. J. S., and Dardenne, M. A., 2012. U–Pb and Hf isotope study on detrital zircons from the Paranoá Group, Brasília Belt Brazil: Constraints on depositional age at Mesoproterozoic–Neoproterozoic transition and tectono-magmatic events in the São Francisco craton. Precambrian Research, 206, 168-181.

Misi, A., Iyer, S. S., Coelho, C. E. S., Tassinari, C. C. G., Franca-Rocha, W. J. S., Cunha, I. A., Gomes, A. S. R., Oliveira, T. F., Teixeira, J. B. G., Filho, V. M., 2005. Sediment hosted lead–zinc deposits of the Neoproterozoic Bambuí Group and correlative sequences, São Francisco Craton, Brazil: a review and a possible metallogenic evolution model. Ore Geology Reviews 26, 263–304.

Misi, A., Kaufman, A. J., Veizer, J., Powis, K., Azmy, K., Boggiani, P. C., Gaucher, C., Teixeira, J. B. G., Sanches, A. L., Iyer, S. S. S., 2007. Chemostratigraphic correlation of Neoproterozoic successions in South America. Chemical Geology 237 (2007) 143–167.

Misi, A., Kaufman, A. J., Azmy, K., Dardenne, M. A., Sial, A. N., and de Oliveira, T. F., 2011. Neoproterozoic successions of the São Francisco craton, Brazil: the Bambuí, Una, Vazante and Vaza Barris/Miaba groups and their glaciogenic deposits. Geological Society, London, Memoirs, 36(1), 509-522.

Monteiro, L. V. S., Bettencourt, J. S., Bello, R. M. S., Juliani, C., Tassinari, C. C. G., Oliveira, T. F., and Pérez-Aguillar, A., 2003. Sulfur, carbon, oxygen and strontium isotopic evidences for the genesis of the hydrothermal zinc non-sulfide and sulfide mineralizations in the Vazante, Ambrosia and Fagundes deposits, MG, Brazil. In Short Papers IV South American Symposium on Isotope Geology, 748-751.

Monteiro, L. V. S., Bettencourt, J. S., Juliani, C., and de Oliveira, T. F., 2006. Geology, petrography, and mineral chemistry of the Vazante non-sulfide and Ambrósia and Fagundes sulfide-rich carbonate-hosted Zn–(Pb) deposits, Minas Gerais, Brazil. Ore Geology Reviews, 28(2), 201-234.

Olcott, A. N., Sessions, A. L., Corsetti, F. A., Kaufman, A. J., and De Oliviera, T. F., 2005. Biomarker evidence for photosynthesis during Neoproterozoic glaciation. Science, 310(5747), 471-474.

Paula-Santos, G.M., 2013. Quimioestratigrafia isotópica (C, O, Sr) e geocronologia (U-Pb, Sm-Nd) das rochas da Formação Sete Lagoas, Grupo Bambuí. Master Thesis, University of São Paulo. São Paulo, 142 p..

Pedrosa-Soares, A. C., Cordani, U. and Nutman, A., 2000. Constraining the age of Neoproterozoic glaciation in eastern Brazil: first U-Pb (SHRIMP) data from detritalzircons. Revista Brasileira de Geociências 30, 58-61.

Pereira, L. F., Dardenne, M. A., Rosière, C. A., and Pedrosa-Soares, A. C., 1994. Evolução geológica dos grupos Canastra e Ibia na região entre Coromandel e Guarda-Mor, MG. Revista Geonomos, 2(1), 22-32.

Peters, K. E., and Cassa, M. R., 1994. Applied source rock geochemistry. Memoirs-American Association of Petroleum Geologists, 93-93.

Peucker-Ehrenbrink, B., and Jahn, B. M., 2001. Rhenium-osmium isotope systematics and platinum group element concentrations: Loess and the upper continental crust. Geochemistry, Geophysics, Geosystems, 2(10).

Pimentel, M. M., Fuck, R. A., and Botelho, N. F., 1999. Granites and the geodynamic history of the Neoproterozoic Brasılia Belt, central Brazil: a review. Lithos, 46(3), 463-483.

Pimentel, M., Dardenne, M., Fuck, R., Viana, M., Junges, S. L., Fischel, D. P., Seer, H.J., and Dantas, E. L., 2001. Nd isotopes and the provenance of detrital sediments of the Neoproterozoic Brasılia Belt, central Brazil. Journal of South American Earth Sciences, 14(6), 571-585.

Pimentel, M. M., Rodrigues, J. B., DellaGiustina, M. E. S., Junges, S., Matteini, M., and Armstrong, R., 2011. The tectonic evolution of the Neoproterozoic Brasília Belt, central Brazil, based on SHRIMP and LA-ICPMS U–Pb sedimentary provenance data: A review. Journal of South American Earth Sciences, 31(4), 345-357.

Ravizza, G., and Turekian, K. K., 1989. Application of the ^{187}Re-^{187}Os system to black shale geochronometry. Geochimica et Cosmochimica Acta, 53(12), 3257-3262.

Rodrigues, J. B., 2008. Proveniência de sedimentos dos grupos Canastra, Ibiá, Vazante e Bambuí e Um estudo de zircões detríticos e Idades Modelo Sm-Nd. Doctoral Thesis, University of Brasília. Brasília, 141 p..

Rodrigues, J. B., Pimentel, M. M., Dardenne, M. A., and Armstrong, R. A., 2010. Age, provenance and tectonic setting of the Canastra and Ibiá Groups (Brasília Belt, Brazil): Implications for the age of a Neoproterozoic glacial event in central Brazil. Journal of South American Earth Sciences, 29(2), 512-521.

Rodrigues, J. B., Pimentel, M. M., Buhn, B., Matteini, M., Dardenne, M. A., Alvarenga, C. J. S., and Armstrong, R. A., 2012. Provenance of the Vazante Group: New U–Pb, Sm–Nd, Lu–Hf isotopic data and implications for the tectonic evolution of the Neoproterozoic Brasília Belt. Gondwana Research, 21(2), 439-450.

Rooney, A. D., Selby, D., Houzay, J. P., and Renne, P. R., 2010. Re–Os geochronology of a Mesoproterozoic sedimentary succession, Taoudeni Basin, Mauritania: Implications for basin-wide correlations and Re–Os organic-rich sediments systematics. Earth and Planetary Science Letters, 289(3), 486-496.

Rooney, A. D., Chew, D. M., and Selby, D., 2011. Re–Os geochronology of the Neoproterozoic–Cambrian Dalradian supergroup of Scotland and Ireland:

implications for Neoproterozoic stratigraphy, glaciations and Re–Os systematics. Precambrian Research, 185(3), 202-214.

Rooney, A. D., Macdonald, F. A., Strauss, J. V., Dudás, F. Ö., Hallmann, C., Selby, D., 2014. Re-Os Geochronology and coupled Os-Sr isotope constraints on the Sturtian snowball Earth. Proceedings of the National Academy of Sciences, 111, 51-56.

Rubo, R. A., and Monteiro, L. V. S., 2010. Sistemática de isótopos de oxigênio e carbono aplicada ao estudo da evolução metalogenética do depósito de Zn-Pb de Morro Agudo (MG). Brazilian Journal of Geology, 40(3), 438-452.

Santos, R. V., De Alvarenga, C. J. S., Dardenne, M. A., Sial, A. N., and Ferreira, V. P., 2000. Carbon and oxygen isotope profiles across Meso-Neoproterozoic limestones from central Brazil: Bambuí and Paranoá groups. Precambrian Research, 104(3), 107-122.

Selby, D., and Creaser, R. A., 2003. Re–Os geochronology of organic rich sediments: an evaluation of organic matter analysis methods. Chemical Geology, 200(3), 225-240.

Selby, D., and Creaser, R. A., 2005a. Direct radiometric dating of the Devonian-Mississippian time-scale boundary using the Re-Os black shale geochronometer. Geology, 33(7), 545-548.

Selby, D., and Creaser, R. A., 2005b. Direct radiometric dating of hydrocarbon deposits using rhenium-osmium isotopes. Science, 308(5726), 1293-1295.

Selby, D., Creaser, R. A., Dewing, K., and Fowler, M., 2005. Evaluation of bitumen as a ^{187}Re–^{187}Os geochronometer for hydrocarbon maturation and migration: A test case from the Polaris MVT deposit, Canada. Earth and Planetary Science Letters, 235 (1), 1-15.

Selby, D., 2007. Direct Rhenium-Osmium age of the Oxfordian-Kimmeridgian boundary, Staffin bay, Isle of Skye, UK, and the Late Jurassic time scale. Norsk Geologisk Tidsskrift, 87(3), 291-299.

Smoliar, M.I., Walker, R.J., Morgan, J.W., 1996. Re-Os isotope constraints on the age of Group IIA, IIIA, IVA, and IVB iron meteorites. Science 271, 1099-1102.

Sperling, E.A., Rooney, A.D., Hays, L., Sergeev, V.N., Vorob'eva, N.G., Sergeeva, N.D., Selby, D., Johnston, D.T., and Knoll, A.H., 2014. Redox heterogeneity of subsurface waters in the Mesoproterozoic ocean. Geobiology. DOI:10.1111/gbi.12091.

Tonietto, S. N., 2011. Diagênese e hidrotermalismo em rochas carbonáticas proterozóicas: Grupos Bambuí e Vazante, Bacia do São Francisco. Master Thesis. University of Brasília. Brasília, 196 p..

Uhlein, A., Trompette, R. R., Egydio-Silva, M., Vauhez, M., 2007. A glaciação Sturtiana (~750 Ma), a estrutura do rifte Macaúbas Santo Onofre e a estratigrafia do

Grupo Macaúbas, Faixa Araçuaí. Revista Geonomos, 15, 45-60.

Valeriano, C. M., Machado, N., Simonetti, A., Valladares, C. S., Seer, H. J., Simões, L. S. A., 2004. U-Pb geochronology of the Southern Brasília Belt (SE-BRAZIL): sedimentary provenance, Neoproterozoic Orogeny and assembly of West Gondwana. Precambrian Research 130, 27-55.

Valeriano, C. M., Pimentel, M. M., Heilbron, M., Almeida, J. C. H., Trouw, R. A. J., 2008. Tectonic evolution of the Brasília Belt, central Brazil, and early assembly of Gondwana. In: Pankhurst, R.J., Trouw, R.A.J., Brito Neves, B.B., De Wit, M.J. (Eds.), West Gondwana: Pre-cenozoic Correlations across the South Atlantic Region. Geological Society, London, Special Publications, 294, 197-210.

van Acken, D., Thomson, D., Rainbird, R. H., and Creaser, R. A., 2013. Constraining the depositional history of the Neoproterozoic Shaler Supergroup, Amundsen Basin, NW Canada: Rhenium-osmium dating of black shales from the Wynniatt and Boot Inlet Formations. Precambrian Research, 236, 124-131.

Vieira, L. C., Almeida, R. P., Trindade, R. I., Nogueira, A. C., and Janikian, L., 2007. A Formação Sete Lagoas em sua área-tipo: fácies, estratigrafia e sistemas deposicionais. Revista Brasileira de Geociências, 37 (4), 1-14.

Warren, L. V., Quaglio, F., Riccomini, C., Simões, M. G., Poiré, D. G., Strikis, N. M., Anelli L.E., and Strikis, P. C., 2014. The puzzle assembled: Ediacaran guide fossil Cloudina reveals an old proto-Gondwana seaway. Geology, 42(5), 391-394.

Zalán, P. V., and Silva, P. C. R., 2007. Bacia do São Francisco. Boletim de Geociências da Petrobrás, 15(2), 561-571.

Figure Captions

Fig. 1. Location and geology of the study area. (A) São Francisco Craton, São Francisco Basin and surrounding belts (BFB=Brasilia Fold Belt); (B) Simplified geological map of the Brasília Belt (after Dardenne, 2000).

Fig. 2. Lithostratigraphic column of the Canastra Group (modified from Dardenne, 2000). Youngest concordant age interpreted as maximum depositional age: [1]Rodrigues et al. (2010); [2]Dias, 2011; [3] Valeriano (2004). Average thickness from Pereira et al. (1994).

Fig. 3. Lithostratigraphic column of the Vazante Group (modified from Dardenne, 2000). Youngest concordant age interpreted as maximum depositional age: [1]Rodrigues et al. (2012); Re-Os isochron interpreted as depositional age: [2]Geboy (2006); [3]Azmy et al. (2008); [4]Geboy et al. (2013). Average thickness from Misi et al. (2011).

Fig. 4. Lithostratigraphic column of the Bambuí Group (modified from Dardenne, 2000). Youngest concordant age interpreted as maximum depositional age: [1]Rodrigues (2008); [3]Paula-Santos (2013). Pb-Pb isochron interpreted as depositional age: [2]Babinski et al. (2007). Index fossil *Cloudina*: [4]Warren et al. (2014). Average thickness from Vieira et al. (2007).

Fig. 5. Stratigraphic levels used for TOC and Re–Os measurements (A) Paracatu Formation, drillhole MASW03; (B) Serra do Garrote Formation, drillcore VZCF001;

(C) Sete Lagoas Formation, drillcore LMR1009.

Fig. 6. Re–Os isochron diagram (A) Paracatu Formation organic-rich slates, drillhole MASW03; (B) Serra do Garrote Formation organic-rich slates, drillhole VZCF001.

Tables

Table 1: TOC content for the Canastra, Vazante and Bambuí groups.

Table 2: Re-Os isotope data for the Paracatu and Serra do Garrote formations. *Rho is the associated error correlation at 2σ (Ludwig, 1980). $^{\S}Os_i$ is the initial $^{187}Os/^{188}Os$ isotope ratio calculated at 1002 Ma for the Paracatu Formation and 1300 Ma for the Serra do Garrote Formation. VZCF-6r is a repeat analysis and was not included in the regression

Sample	Re (ppb)	±	Os	±	$^{187}Re/^{188}Os$	±	$^{187}Os/^{188}Os$	±	Rho*	Osi§
Paracatú										
MASW03-36	0.30	0.001	64.8	1.2	24.2	0.3	0.667	0.038	0.705	0.260
MASW03-38	0.36	0.001	52.7	1.0	36.1	0.7	0.847	0.030	0.705	0.239
MASW03-40	4.11	0.013	296.5	2.1	79.6	0.8	1.593	0.040	0.656	0.253
MASW03-42	1.31	0.004	175.1	1.0	39.8	0.6	0.934	0.030	0.654	0.264
Serra do Garrote										
VZCF001-6	18.7	0.06	507.2	5.2	317.9	2.8	6.167	0.070	0.656	-0.793
VZCF001-6r	18.9	0.06	515.7	9.3	314.3	6.4	6.136	0.174	0.698	-0.746
VZCF001-11	9.2	0.03	260.2	2.5	269.9	2.4	4.654	0.053	0.657	-1.255
VZCF001-13	28.3	0.09	584.6	7.0	601.2	5.2	12.207	0.139	0.656	-0.956
VZCF001-3	4.0	0.01	136.8	2.2	205.1	4.2	3.628	0.103	0.699	-0.862

Formation	Sample	Depth [m]	TOC [wt%]
Serra do Garrote	VZCF001-1	280.23	0.85
	VZCF001-2	281.33	1.53
	VZCF001-3	281.55	0.07
	VZCF001-4	281.78	2.15
	VZCF001-5	282.00	0.87
	VZCF001-6	282.23	2.10
	VZCF001-7	285.78	0.72
	VZCF001-8	286.63	0.20
	VZCF001-9	287.78	0.93
	VZCF001-10	288.43	1.48
	VZCF001-11	288.98	0.62
	VZCF001-12	289.15	1.98
	VZCF001-13	289.60	1.50
	VZCF001-14	289.98	1.38
	VZCF001-15	292.55	1.89
Paracatú	MASW03-33	47.6	2.12
	MASW03-34	48.0	1.76
	MASW03-35	48.3	1.75
	MASW03-36	48.6	1.56
	MASW03-37	49.9	1.48
	MASW03-38	50.4	1.03
	MASW03-39	50.7	1.42
	MASW03-40	51.0	0.92
	MASW03-41	52.3	1.23
	MASW03-42	52.6	1.19
	MASW03-43	52.9	1.16
	MASW03-44	53.2	0.99
	MASW03-45	53.5	1.59
	MASW03-46	55.6	0.75
	MASW03-47	55.9	1.13
Sete Lagoas	LIMR1009-U4S15	35.85	0.08
	LIMR1009-U4S14	36.85	0.17
	LIMR1009-U4S13	37.85	0.03
	LIMR1009-U4S12	38.85	0.05
	LIMR1009-U4S11	39.85	0.02
	LIMR1009-U4S10	40.85	0.04
	LIMR1009-U4S9	41.85	0.02
	LIMR1009-U4S8	42.85	0.04
	LIMR1009-U4S7	43.85	0.10
	LIMR1009-U4S6	44.85	0.03
	LIMR1009-U4S5	45.85	0.04
	LIMR1009-U4S4	46.25	0.02
	LIMR1009-U4S3	46.65	0.01
	LIMR1009-U4S2	47.05	0.02
	LIMR1009-U4S1	47.57	0.01
	LIMR1009-U3S8	112.34	0.01
	LIMR1009-U3S7	113.34	0.01
	LIMR1009-U3S6	114.34	0.02
	LIMR1009-U3S5	115.34	0.08
	LIMR1009-U3S4	116.34	0.01
	LIMR1009-U3S3	116.74	0.04
	LIMR1009-U3S2	117.14	0.03
	LIMR1009-U3S1	117.54	0.02
	LIMR1009-U2S15	145.75	0.00
	LIMR1009-U2S14	146.75	0.00
	LIMR1009-U2S13	147.75	0.00
	LIMR1009-U2S12	148.75	0.02
	LIMR1009-U2S11	149.75	0.00
	LIMR1009-U2S10	150.75	0.02
	LIMR1009-U2S9	151.75	0.08
	LIMR1009-U2S8	152.75	0.00

LIMR1009-U2S7	153.75	0.01
LIMR1009-U2S6	154.75	0.01
LIMR1009-U2S5	155.75	0.00
LIMR1009-U2S4	156.15	0.01
LIMR1009-U2S3	156.55	0.06
LIMR1009-U2S2	156.95	0.02
LIMR1009-U2S1	157.35	0.13
LIMR1009-U1S1	158.15	0.32
LIMR1009-U1S2	158.55	0.22
LIMR1009-U1S3	158.95	0.24
LIMR1009-U1S4	159.35	0.24
LIMR1009-U1S5	159.75	0.22
LIMR1009-U1S6	160.75	0.06
LIMR1009-U1S7	161.75	0.36
LIMR1009-U1S8	162.75	0.14
LIMR1009-U1S9	163.75	0.49
LIMR1009-U1S10	164.75	0.33

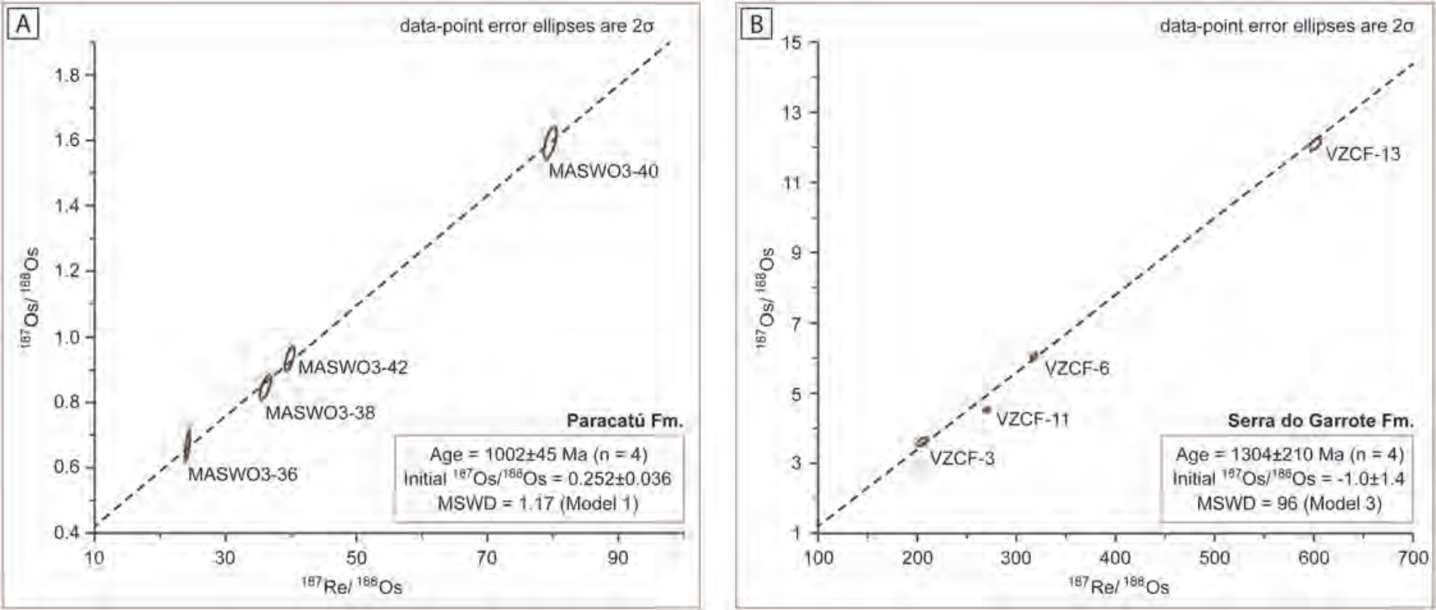
A
data-point error ellipses are 2σ
MASWO3-40
MASWO3-42
MASWO3-38
MASWO3-36
Paracatú Fm.
Age = 1002±45 Ma (n = 4)
Initial 187Os/188Os = 0.252±0.036
MSWD = 1.17 (Model 1)
187Os/188Os
187Re/188Os
B
data-point error ellipses are 2σ
VZCF-13
VZCF-6
VZCF-11
VZCF-3
Serra do Garrote Fm.
Age = 1304±210 Ma (n = 4)
Initial 187Os/188Os = -1.0±1.4
MSWD = 96 (Model 3)
187Os/188Os
187Re/188Os

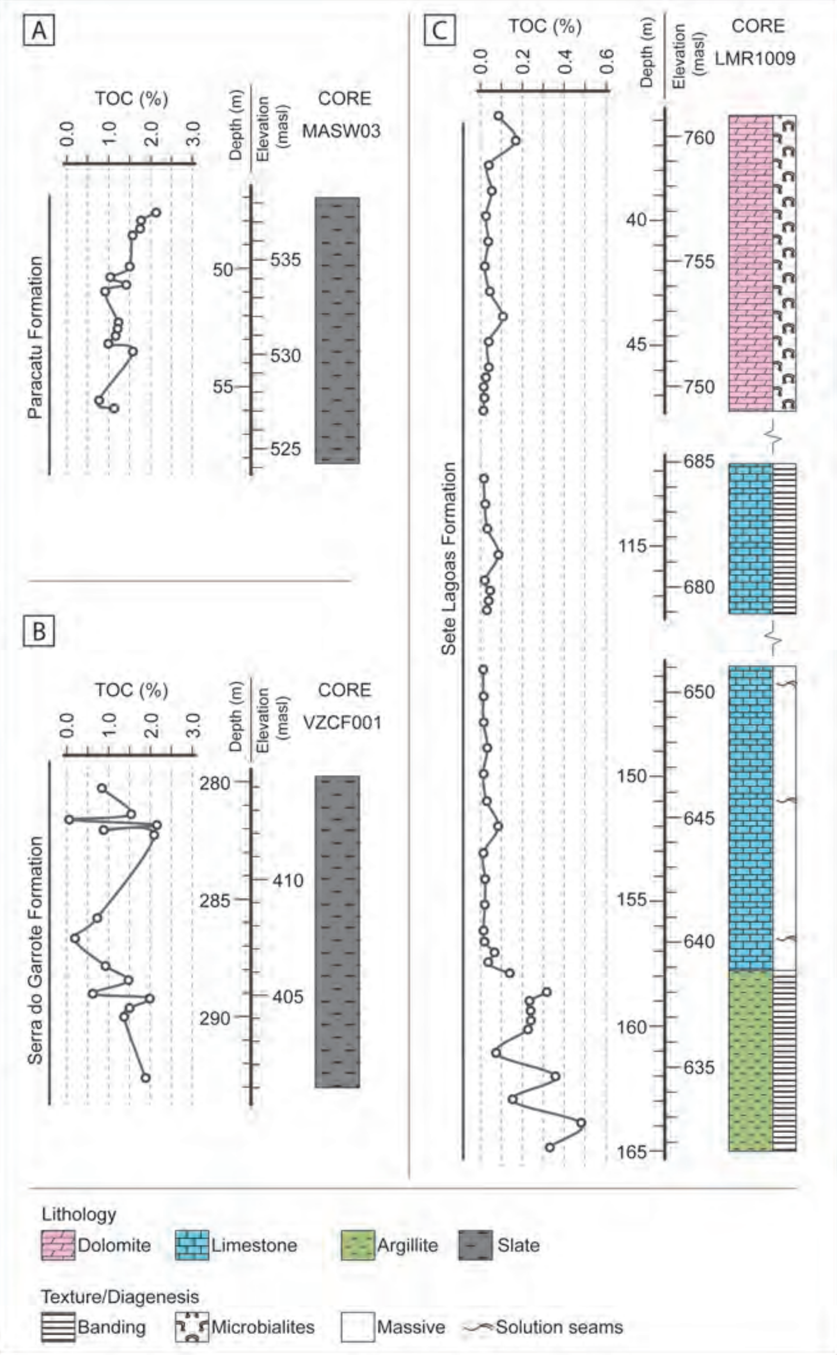
A
TOC (%)
0.0
1.0
2.0
3.0
Depth (m)
Elevation (masl)
CORE
MASW03
Paracatu Formation
50
55
535
530
525
B
TOC (%)
Depth (m)
Elevation (masl)
CORE
VZCF001
Serra do Garrote Formation
280
285
290
410
405
C
TOC (%)
0.0
0.2
0.4
0.6
Depth (m)
Elevation (masl)
CORE
LMR1009
Sete Lagoas Formation
760
40
755
45
750
685
115
680
650
150
645
155
640
160
635
165
Lithology
Dolomite
Limestone
Argillite
Slate
Texture/Diagenesis
Banding
Microbialites
Massive
Solution seams

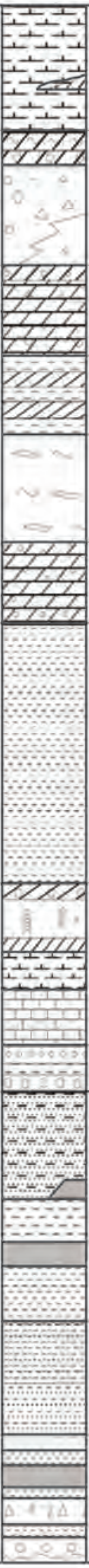

Group	Formation	Lithology	Youngest concordant age (Ma)	Depositional age (Ma)
VAZANTE (~5000 m thick)	Lapa	Carbonaceous phyllite, carbonatic metasiltstone quartzites, conglomerate and slate	1084±14 (1)	
	Morro do Calcário	Dolomitic biostromes and bioherms, breccia, dolorudite, oolitic dolarenite and oncolits	1137±8 (1)	993±46 (3) 1100±77 (3) 1112±50 (4)
	Serra do Poço Verde	Limestones with stromatolitic mats and mud crack		1126±47 (2)
		Slate with intercalations of dolomite		
		Dolomite with stromatolitic mats and bird's eyes		
		Dolomite with layers of breccias and doloarenite		
	Serra do Garrote	Carbonaceous pyrite-bearing slate with rare fine quartzite intercalations	1296±13 (1)	1353±69 (2) 1354±88 (4)
	Lagamar	Stromatolitic bioherma interdigitated with carbonate-bearing metasiltstone and slate. Intraformational dolomitic breccia.		
		Conglomerate, quartzite, metasiltstone and slate		
	Rocinha	Phophoarenite rich in intraclasts and pellet	935±14 (1)	
		Slate, with pyrite and phosphorite		
		Rhythmic package of slate and metasiltstone		
	Santo Antonio do Bonito/Retiro	Quartzite, intercalated with slate. Diamictite	997±29 (1)	

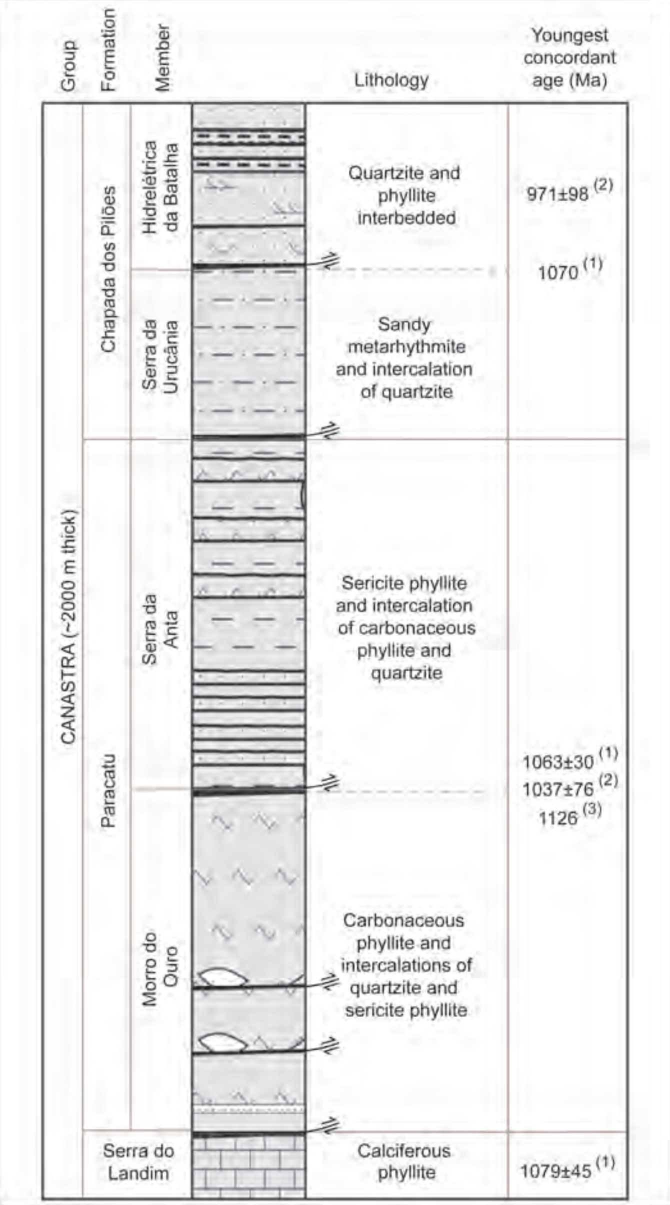

Group
Formation
Member
Lithology
Youngest concordant age (Ma)
CANASTRA (~2000 m thick)
Chapada dos Pilões
Hidrelétrica da Batalha
Quartzite and phyllite interbedded
971±98 (2)
1070 (1)
Serra da Urucânia
Sandy metarhythmite and intercalation of quartzite
Paracatu
Serra da Anta
Sericite phyllite and intercalation of carbonaceous phyllite and quartzite
1063±30 (1)
1037±76 (2)
1126 (3)
Morro do Ouro
Carbonaceous phyllite and intercalations of quartzite and sericite phyllite
Serra do Landim
Calciferous phyllite
1079±45 (1)

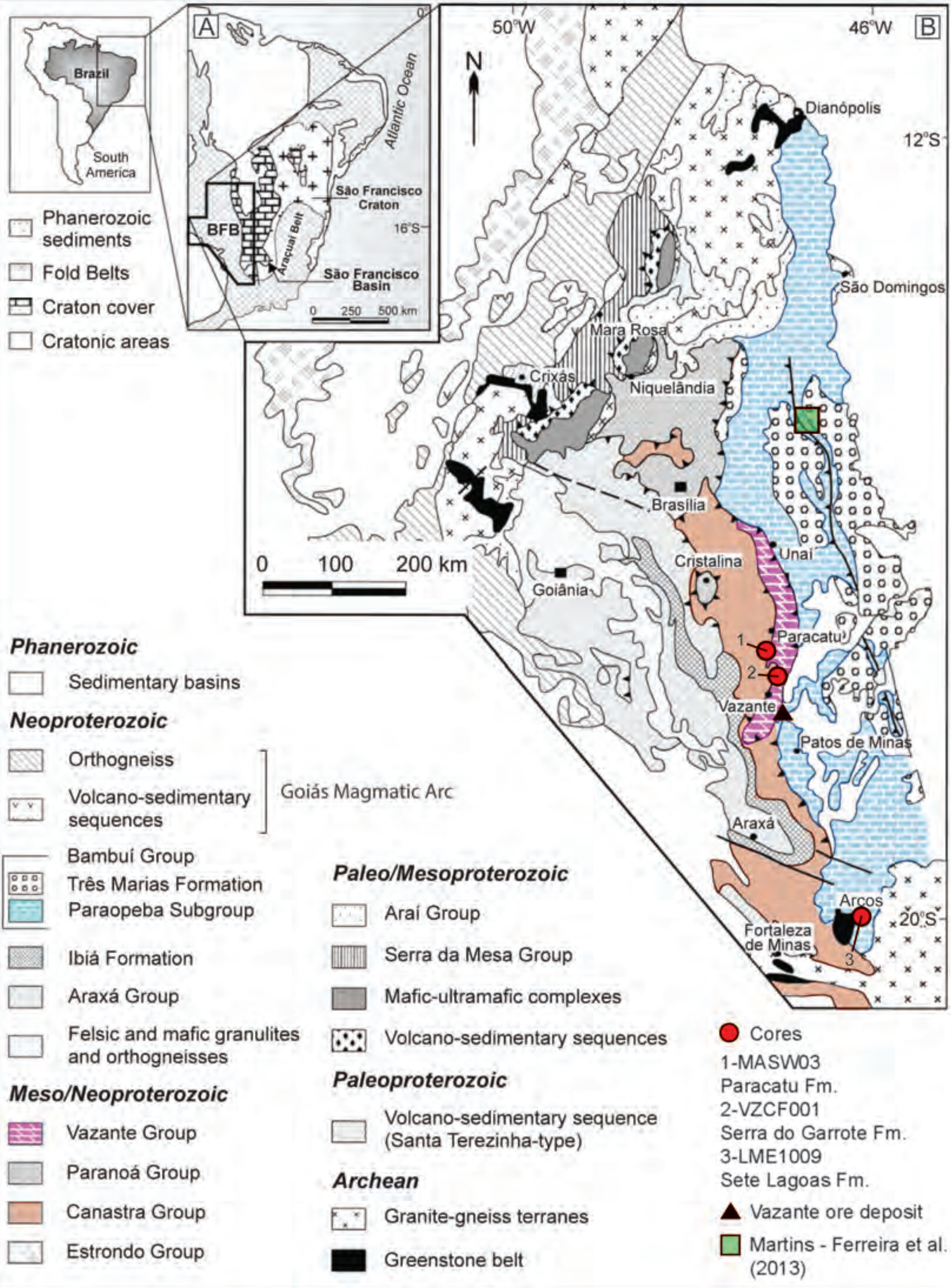

A
B
Brazil
South America
Atlantic Ocean
São Francisco Craton
BFB
Araçuaí Belt
16°S
São Francisco Basin
0 250 500 km
Phanerozoic sediments
Fold Belts
Craton cover
Cratonic areas
50°W
46°W
N
12°S
20°S
Dianópolis
São Domingos
Mara Rosa
Crixás
Niquelândia
Brasília
Cristalina
Unaí
Goiânia
Paracatu
Vazante
Patos de Minas
Araxá
Arcos
Fortaleza de Minas
0 100 200 km
1
2
3
Phanerozoic
Sedimentary basins
Neoproterozoic
Orthogneiss
Volcano-sedimentary sequences
Goiás Magmatic Arc
Bambuí Group
Três Marias Formation
Paraopeba Subgroup
Ibiá Formation
Araxá Group
Felsic and mafic granulites and orthogneisses
Meso/Neoproterozoic
Vazante Group
Paranoá Group
Canastra Group
Estrondo Group
Paleo/Mesoproterozoic
Araí Group
Serra da Mesa Group
Mafic-ultramafic complexes
Volcano-sedimentary sequences
Paleoproterozoic
Volcano-sedimentary sequence (Santa Terezinha-type)
Archean
Granite-gneiss terranes
Greenstone belt
Cores
1-MASW03
Paracatu Fm.
2-VZCF001
Serra do Garrote Fm.
3-LME1009
Sete Lagoas Fm.
Vazante ore deposit
Martins - Ferreira et al. (2013)